

# Effects of texture and grain size on mechanical properties of AZ80 magnesium alloys at lower temperatures

Lifei Wang<sup>a,\*</sup>, Ehsan Mostaed<sup>b</sup>, Xiaoqing Cao<sup>a</sup>, Guangsheng Huang<sup>c</sup>, Alberto Fabrizi<sup>d</sup>, Franco Bonollo<sup>d</sup>, Chengzhong Chi<sup>a</sup>, Maurizio Vedani<sup>b</sup>

<sup>a</sup> College of Material Science and Engineering, Taiyuan University of Technology, 030024 Taiyuan, China

<sup>b</sup> Department of Mechanical Engineering, Politecnico di Milano, 20156 Milan, Italy

<sup>c</sup> College of Material Science and Engineering, Chongqing University, 400030 Chongqing, China

<sup>d</sup> Department of Management and Engineering, Università di Padova, Stradella S. Nicola 3, 36100 Vicenza, Italy

In order to investigate the effect of texture and grain size on mechanical properties of AZ80 magnesium alloy at lower temperatures, ECAP was conducted for 1, 2 and 4 passes at 523 K. Tensile and compressive tests were carried out on the ECAP processed samples at room temperature, 373 K and 423 K, respectively. The results showed that a significant grain refinement took place and the original extrusion fiber texture evolved into a new pre-ferred crystal orientation, featuring a favorable alignment of the basal planes along shear planes after ECAP process. At room temperature grain refinement strengthening played an important role, leading to an improvement of mechanical properties with increasing number of ECAP passes. However, at higher temperature, texture and grain boundary sliding (GBS) mechanisms controlling deformation behaviors, resulting in a softening effect and considerable fracture elongation improvement, as well as yield asymmetry reduction.

Keywords: AZ80 magnesium alloy ECAP, Asymmetry, Texture, Grain size

## 1. Introduction

As the lightest metallic materials for structural applications, Mg alloys are considered to be promising candidates having great potential in electronic, automotive, aerospace and biomedical applications due to their high specific strength and stiffness, damping properties and recyclability [1,2]. However, owing to its hexagonal close packed (HCP) structure, magnesium shows poor ductility at room temperature (RT). That is, since Mg exhibits inadequate number of available slipping systems at low temperatures, the *Von Mises Criterion* requiring at least 5 independent slip systems for extensive plasticity cannot be satisfied [3]. Accordingly, Mg expresses rather poor mechanical properties and formability at RT. It is accepted that grain refinement improves the aforementioned properties of Mg alloys [4,5,6]. Within this frame, severe plastic deformation (SPD), especially equal channel angular pressing (ECAP), revealed to be one of the most effective grain refining methods for metallic materials. Xia et al. [7] reported that the grain size of AZ31 Mg alloy decreased from 22  $\mu\text{m}$  to less than 1  $\mu\text{m}$  after 8 ECAP passes at 423 K. Lin et al. [8] also confirmed that the grain size of the ZA85 alloy decreased from 150  $\mu\text{m}$  to 1  $\mu\text{m}$  after 6 ECAP passes at 453 K. In

the same research, the authors showed that after ECAP processing, the ultimate tensile strength (UTS) and yield strength (YS) at 473 K of the as-cast ZA85 improved from 105 and 74 MPa to 249 and 162 MPa, respectively. Moreover, the elongation increased from 5.1% to 28.5%. It is also reported that a combination of grain refinement and texture modification, both induced by ECAP, simultaneously play a crucial role in strength and ductility improvement in severely deformed AZ61 Mg alloy [9].

The influence of ECAP processing on RT mechanical properties of Mg alloys has been widely investigated [7,10]. However, the formability of ECAP processed alloys was mainly focused on the high-temperature range, above 473 K [11,12]. It is known that under these conditions additional non-basal slip systems are activated, dynamic recrystallization is readily promoted and the effect of texture is progressively degraded at the same time [13].

To properly evaluate the effect of ECAP on mechanical properties of Mg alloys when only basal slip systems are active (at room and moderate temperature) [14], grain size and the basal texture orientation have to be taken into account simultaneously. In other words, the two mentioned factors have significant impacts on tensile properties measured at levels exceeding the room temperatures but lower than those at which non-basal slip systems start to be activated. For this reason, the present paper is mainly aimed at investigating the mechanical

Article history:

Received 29 July 2015

Received in revised form 24 September 2015

Accepted 28 September 2015

Available online xxxx

\* Corresponding author.

E-mail address: Lifeiwang6@gmail.com (L. Wang).

properties of ECAP processed AZ80 alloy in the warm temperature regime corresponding to values lower than 423 K. In this range, dislocation slip on the basal planes is considered as the only activated slip system.

## 2. Experimental procedures

In this investigation, a commercial as-extruded AZ80 (Mg–8 wt.% Al–0.5 wt.% Zn) alloy was employed. For ECAP processing, cylindrical specimens of 10 mm in diameter with length of 90 mm have been machined from the starting material. ECAP was performed at a temperature of 523 K using a tool steel die with an intersection angle of  $\varphi = 110^\circ$  and an outer arc of curvature of  $\psi = 20^\circ$ . The die was heated by means of four electric resistance heaters (with a power of 1200 W each), thermocouples inserted close to channel intersection region were used to control processing temperature. All samples were pressed using route Bc according to which each billet is rotated in the same direction by  $90^\circ$  around the longitudinal axis after each pass. For these experiments, the billets were sprayed with high temperature lubricant and processed for 1, 2 and 4 passes. Table 1 summarizes the conditions investigated for the AZ80 alloy at the different ECAP passes.

The microstructure of various samples was characterized by optical microscopy, Scanning electron microscopy (SEM) and transmission electron microscopy (TEM). Specimens for TEM observations were prepared by sectioning the ECAP billets perpendicularly to the extrusion direction into 500  $\mu\text{m}$  thickness foils, polishing up to 300  $\mu\text{m}$  using abrasive papers and then punching 3 mm diameter disks.

Finally, the TEM disks were ion milled at room temperature using a PIPS (Precision Ion Polishing System, GATAN™) with a small incident angle until perforation and examined using a JEM 2000 EX II transmission electron microscope operating (JEOL™) at 200 kV and equipped with EDS (Energy Dispersive Spectroscopy, EDAX™). Prior to TEM investigations, the principal phases in the AZ80 alloy were identified using a FEG-SEM (Field Emission Gun Scanning Electron Microscope) Quanta 250-FEI™ with EDS system (EDAX™). The development of texture induced by ECAP was detected by XRD. Finally, the fracture surfaces after tensile tests were observed by SEM.

Tensile specimens were machined along the ECAP direction (ED, corresponding to axial direction of the starting extruded billets) with a gage length of 18 mm and diameter of 4 mm. Compressive samples were cut along axial direction of the as-extruded and ECAP processed billets with diameter and height of 10 mm and 15 mm, respectively. The tests were performed with an electro-mechanical universal testing machine at RT, 373 K and 423 K. During the high-temperature testing, the molds and specimens were heated to the desired temperature by a resistance furnace. Each specimen was kept at the set temperature in the thermostatic chamber fitted to the tensile frame for 5 min before being strained to fracture at an engineering strain rate of  $10^{-3} \text{ s}^{-1}$ .

## 3. Results and discussions

### 3.1. Evolution of microstructure and texture

Fig. 1 shows the microstructure of all the investigated samples observed on the longitudinal section. As seen, as-extruded microstructure consists of equiaxed grains with an average size of 11.2  $\mu\text{m}$ . However,

after 1 ECAP pass, the microstructure of the alloy became bimodal with some relatively large grains, representing the residual part of the original structure having average size of about 10  $\mu\text{m}$ , surrounded by arrays of much smaller grains (Fig. 1b). These new finer grains are supposed to be the result of a dynamic recrystallization (DRX) process that is stimulated by the intense strain and by the processing temperature of 523 K. This phenomenon is consistent with the previous results obtained using AZ31 Mg alloys by Del Valle and Ruano [15].

Fig. 2 shows the SEM micrographs and EDS spectra of particles in 2P and 4P samples, respectively, while Figs. 3 and 4 depict representative TEM images of the same samples for improved grain size evaluation. After 2 passes, the measured average grain size of coarse grains was about 7  $\mu\text{m}$ , while this value increased to 11  $\mu\text{m}$  in case of 4P samples. However, it should be noted that the volume fraction of coarse grains was significantly reduced, resulting in a more equiaxed structure. EDS analyses revealed the chemical composition of two types of intermetallic precipitates. From Fig. 2c and 2d it is inferred that the larger precipitates consist of Mg–Al and Al–Mn suggesting the presence of  $\beta\text{-Mg}_{17}\text{Al}_{12}$  and  $\text{Al}_8\text{Mn}_5$  phases, respectively, while finer particles contain Al and were identified as  $\beta\text{-Mg}_{17}\text{Al}_{12}$  phase. This emergence of the two intermetallic precipitates is consistent with the similar research on AZ80 extrusion process. After extrusion at 250  $^\circ\text{C}$ ,  $\text{Mg}_{17}\text{Al}_{12}$  and  $\text{Al}_8\text{Mn}_5$  occurred in processed Mg alloys [16]. The mentioned small size precipitates might result from the severe deformation process experienced during ECAP leading to fracturing of intermetallic compounds [17]. In addition, most of the fine  $\beta$ -phase particles are located at grain boundaries in the 2P samples, while after 4 passes the area fraction of the particles as well as their average grain size significantly increased, leading to a more homogeneous dispersion of second phase particles in the microstructure.

The TEM micrographs of 2P and 4P samples reported in Figs. 3 and 4, respectively, reveal that within the coarse grains of both samples, needle-like and platelet-like precipitates are formed. According to the literature, they are identified as  $\beta\text{-Mg}_{17}\text{Al}_{12}$  phase [18]. Moreover, the intergranular regions of both materials show a fine microstructure composed of fine  $\alpha$ -Mg equiaxed grains with average sizes of  $\sim 1 \mu\text{m}$ . Small  $\beta$ -phase particles are visible as well mainly located at grain boundaries of finer grains. The small  $\alpha$ -Mg equiaxed grains are probably the result of dynamic recrystallization stimulated during ECAP process [19]. With increasing number of ECAP passes, the volume fraction of finer grains increased and the very fine  $\beta$ -phase particles at grain boundaries was subjected to a coarsening effect in 2P and 4P samples, respectively. The observed precipitate coarsening can be attributed to the relatively high processing temperature (523 K) and relatively long interpass time (estimated to be of about 10 min) during ECAP process.

The (0002) pole figures of investigated samples on their longitudinal section are shown in Fig. 5. As seen, the starting alloy exhibits a typical extrusion direction (ED)  $\parallel <10\text{-}10>$  fiber texture as basal planes in most grains are distributed parallel to the extrusion direction with a maximum texture intensity of 5.78 [20]. After 1 pass of ECAP, the basal planes rotate to ED by  $\sim 10^\circ$  and the maximum texture intensity decreased to 4.49. Then, in 2P samples, the rotation of basal planes to ED becomes more significant and a new texture featuring the alignment of the basal planes along shear direction away from ED appears. However, the strongest component was still the fiber texture with an intensity of 3.79. Eventually, after 4 passes of ECAP, the preferential basal texture orientation ( $45^\circ$ ) became very clear with a considerable divergence and the intensity of (0002) fiber texture further decreased down to 3.3.

Since ECAP processing was undertaken in this investigation using a die with a channel angle of  $110^\circ$ , it is reasonable to anticipate that the basal planes in the majority of grains rearrange during processing to become close to the theoretical shearing plane as the billet passes through the die. The rotation of the (0002) planes close to shearing direction gives rise to a higher Schmid factor of basal slip, leading to easier dislocation movements on the predominant slip plane (0002). In short, the initial fiber texture gradually evolved into a new one featuring the

**Table 1**  
Various condition samples after ECAP on AZ80 magnesium alloys.

Sample code	Sample condition
A	As-received AZ80 alloy
1P	ECAP treated for 1 passes at 523 K
2P	ECAP treated for 2 passes at 523 K
4P	ECAP treated for 4 passes at 523 K



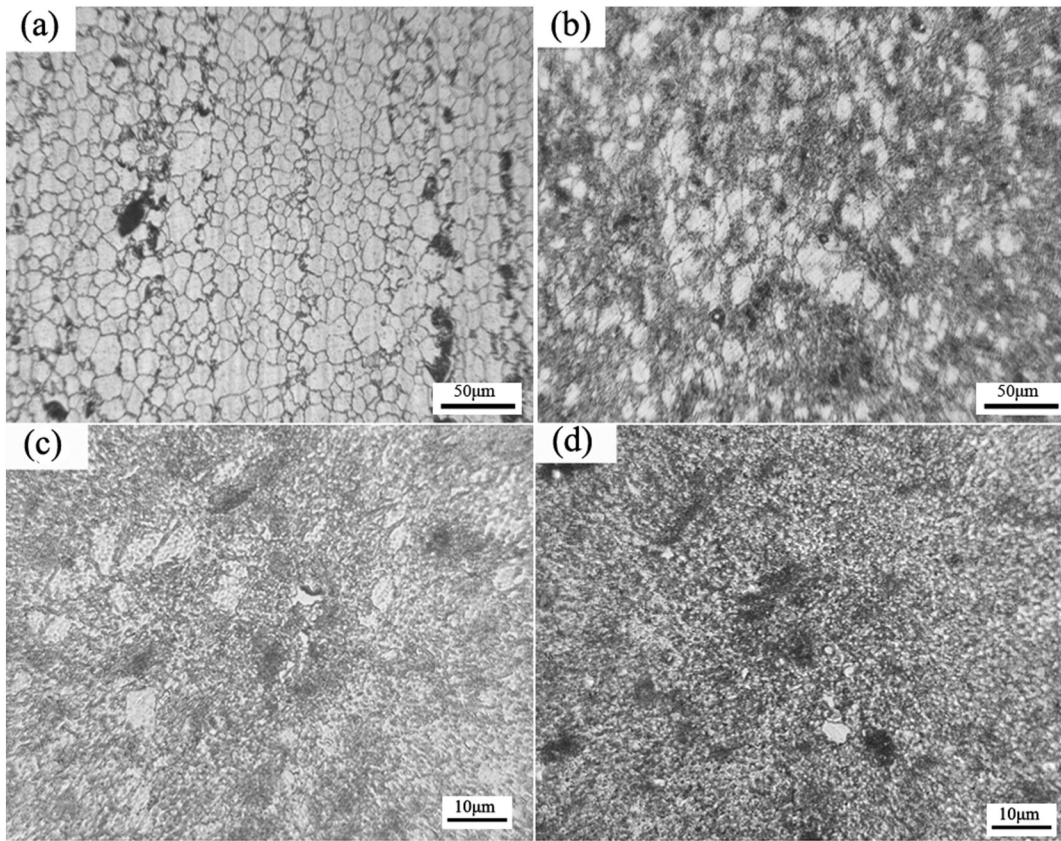


Fig. 1. Microstructure of samples processed to different ECAP passes at 523 K: (a) A, (b) 1P, (c) 2P and (d) 4P samples.

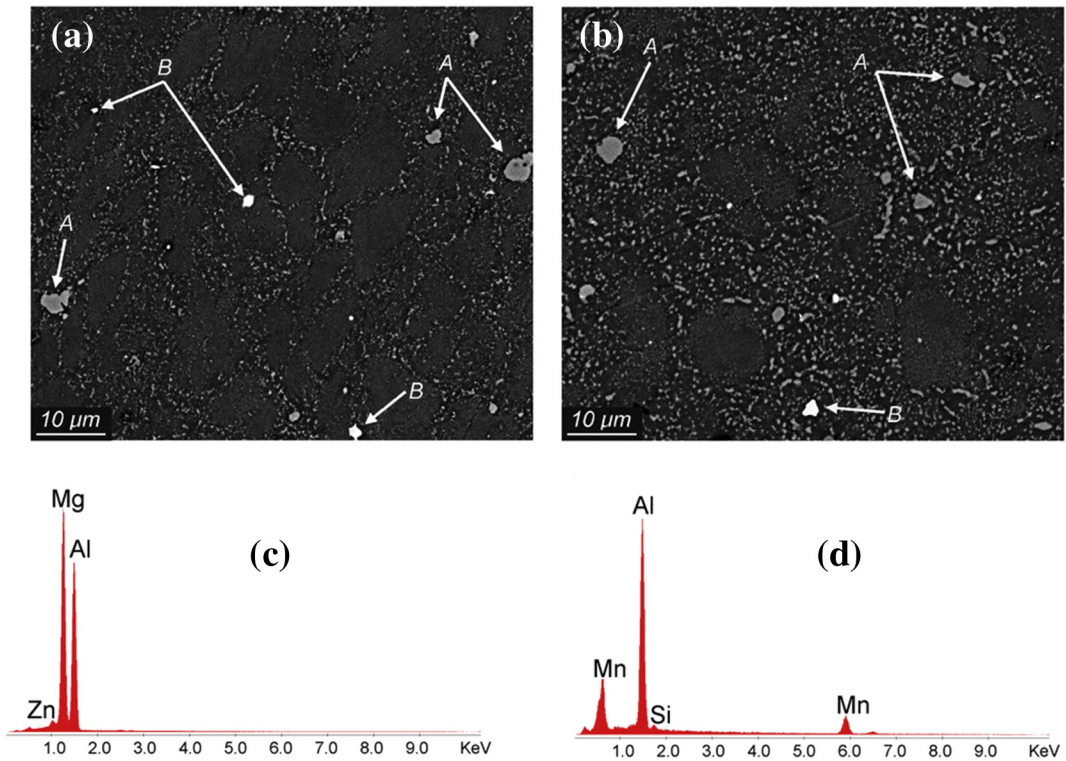
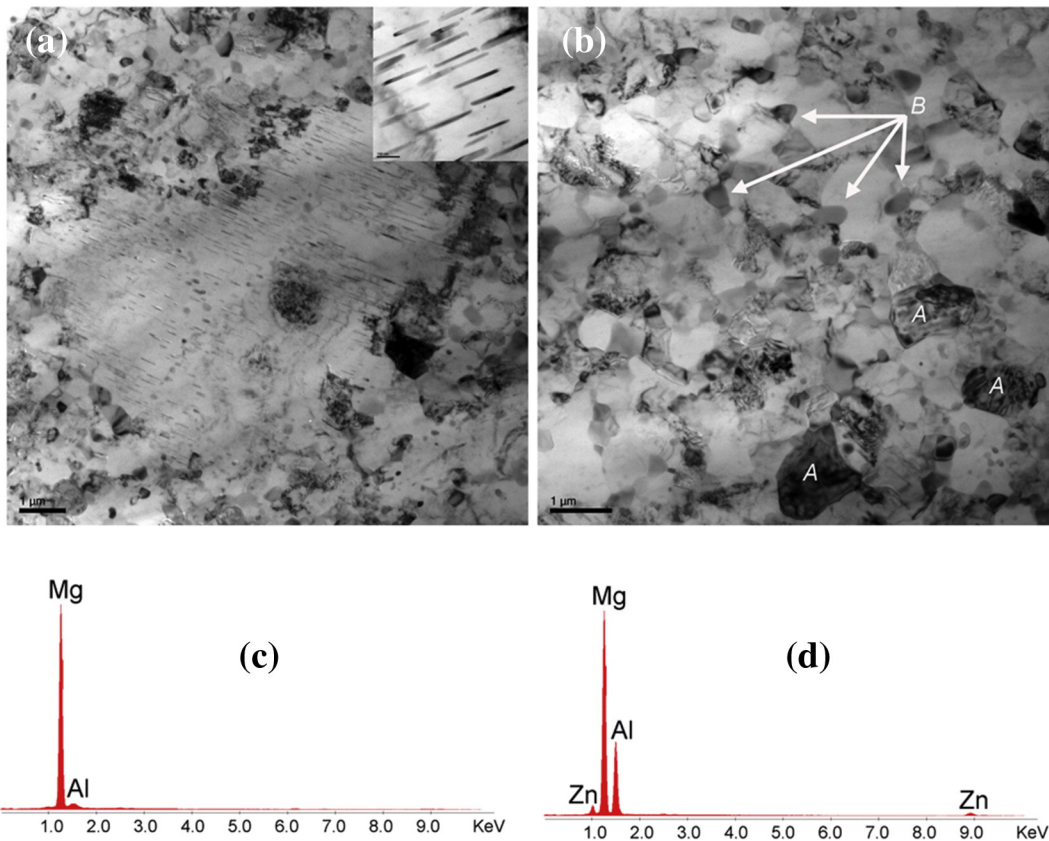


Fig. 2. BSE-SEM micrographs and EDS spectra of particles labeled as A and B in AZ80 alloy ECAPed samples: (a) (c) 2P and (b) (d) 4P.



**Fig. 3.** TEM micrograph of AZ80 microstructure after 2 passes (a): higher magnification: coarse grain of needle-like precipitates in the inset; (b) inter-granular region (c) and (d) EDS spectra of  $\alpha$ -Mg grains (A) and  $\beta$ -phase particles (B).

preferential alignment of the basal planes close to the theoretical ECAP shear planes, featuring a higher Schmid factor value.

### 3.2. Effect of ECAP process on mechanical properties at lower temperatures

Fig. 6 shows the tensile true stress-true strain curves of the AZ80 samples at the three investigated temperatures. At room temperature, as the strain induced by ECAP is enhanced, the flow stress increases and a corresponding minor decrease in measured elongations to failure

can also be observed. The obtained results are consistent with the Hall-Petch relationship whereby the strength increases with decreasing the grain size [21] and they are also consistent with other data reported for cast AZ80 alloy processed by ECAP [22].

As the testing temperature increases to 373 K, the tensile behavior becomes more diffusion-controlled, especially in the regime of plastic flow. The flow stress decreases progressively with increasing numbers of ECAP passes so that the original YS of 253 MPa for the as extruded alloy decreases by 12, 21 and 52 MPa after ECAP by 1, 2 and 4 passes,

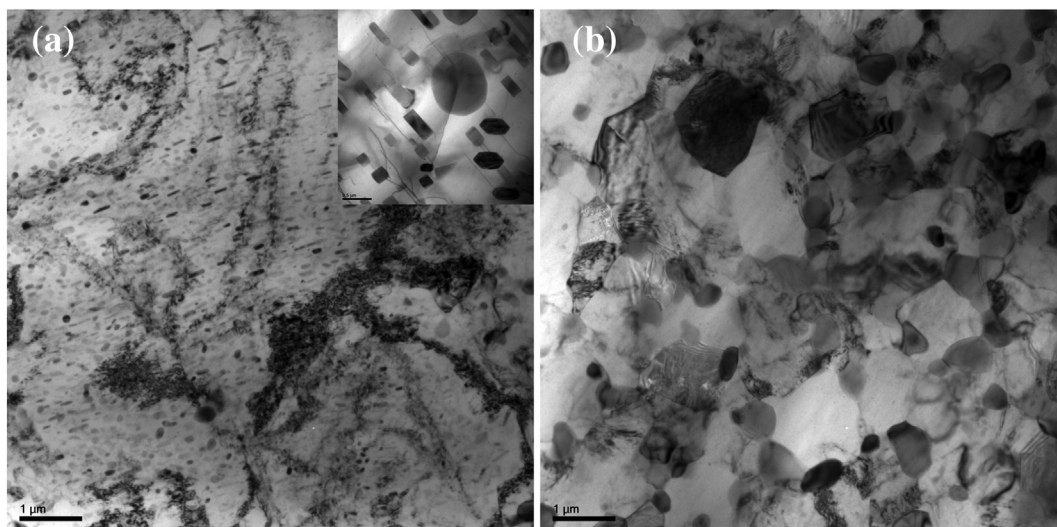


**Fig. 4.** TEM micrograph of AZ80 microstructure after 4 passes: (a) coarse grain with plate-like precipitates as illustrated in the inset; (b) inter-granular region with fine  $\alpha$ -Mg grains with  $\beta$ -phase particles on the grain boundaries.



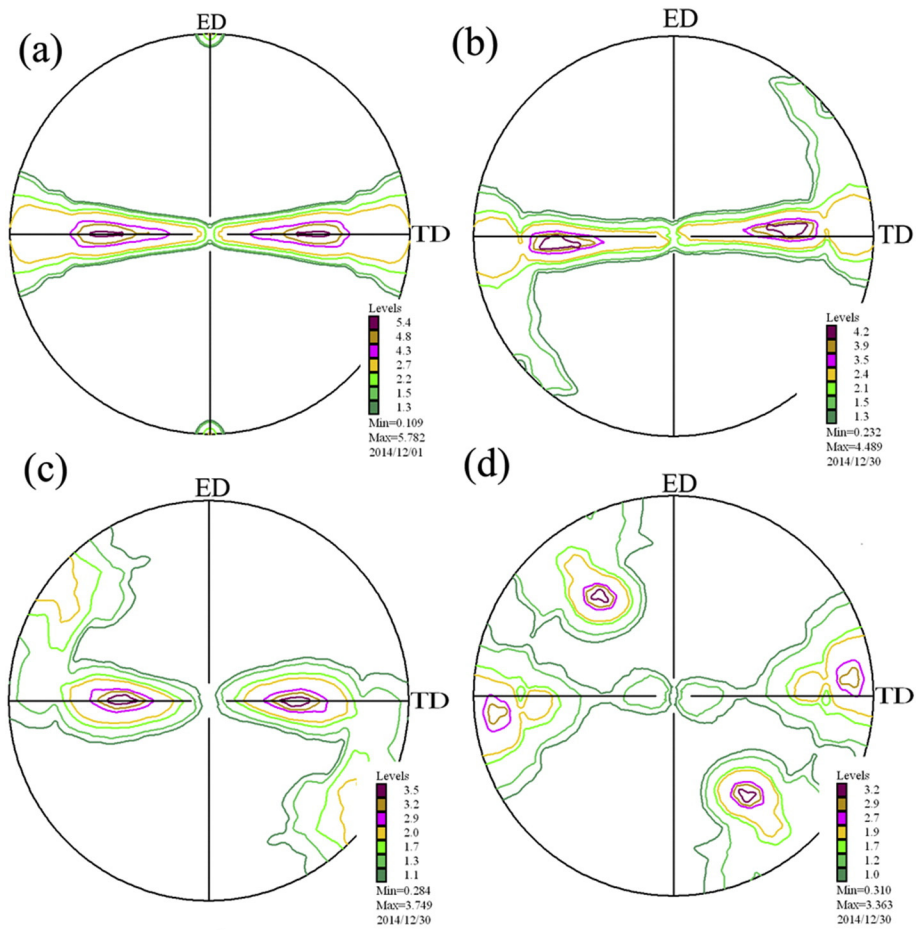


Fig. 5. (0002) pole figure of samples processed by different ECAP passes at 523 K: (a) As-received, (b) 1 pass, (c) 2 passes, (d) 4 passes.

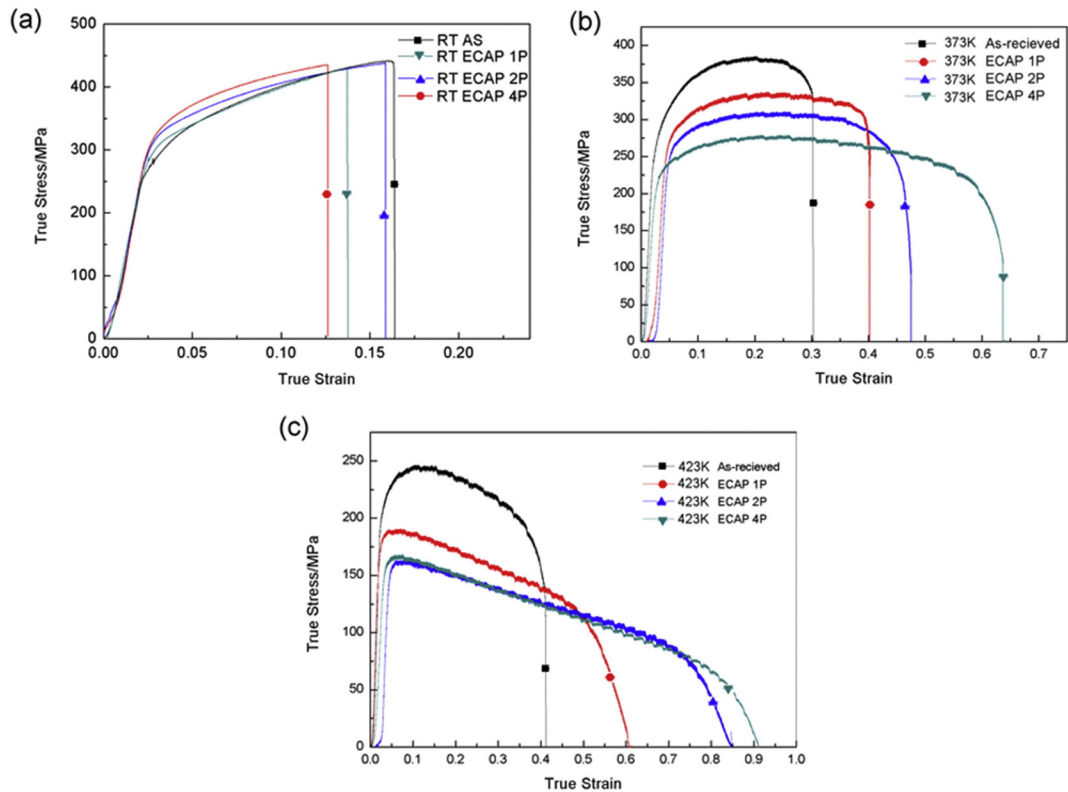


Fig. 6. The tensile true stress vs. true strain curves of AZ80 alloy processed by ECAP at different passes and tested at different temperatures: (a) RT, (b) 373 K, (c) 423 K.

respectively. In addition, the UTS value decreases as ECAP process proceeds, suggesting a trend that is apparently in contrast to the Hall-Petch relationship. The mentioned results indicate that the strength of fine-grained Mg alloy after ECAP is affected not only by the grain size but also by other factors such as dislocation density, texture and grain-boundary structure. Strength dependency on the aforementioned features can be explained by three different observations. First, although expected dislocation density induced by ECAP process is remarkably high, the residual dislocation density decreases more sharply at warm testing conditions, implying that the effect of dislocation strengthening in AZ80 alloy after ECAP becomes less notable [23]. Secondly, at the temperature level of 373 K, texture is believed to play a more important role on the mechanical properties of Mg alloys [24,25]. As shown in Fig. 5, the orientation of basal planes rotated to ED is about  $10^\circ$  after 1 pass of ECAP with a fairly high intensity. Nevertheless, for 2P and 4P, (0002) fiber texture was considerably weakened. Weakening of fiber texture leads to a higher Schmid factor value and this result in easier slip and a lower stress is required for yielding [26,27]. Lastly, the features and size of grains after ECAP may contribute to the grain-boundary sliding (GBS). As well known, GBS becomes more active as the temperature rises. On the other hand, recent research works showed that GBS can be easily operated in finer grains of Mg alloys [28]. GBS is sensitive to the temperature which is enhanced as the temperature increasing. At higher temperature, due to the enhancement activity of GBS in finer grain size microstructure, the plasticity improves and strength decreases as ECAP passes increasing. Koike et al. [29] indicated that non-basal slip systems can be activated in a fine-grained AZ31B alloy, leading to release of the stress concentration, and thereby inducing a concurrent softening effect along with the strengthening caused by grain refinement. GBS and fine grain structure with high Schmid factor value improve the deformation compatibility of grain-boundaries and grains, giving rise to higher ductility.

At 423 K, the strain vs. stress curves express a relatively lower stress and higher fracture elongation compared with those measured at 373 K. This behavior is supposed to be related to the enhanced softening due to dynamic recovery at higher temperatures [30]. With increasing number of ECAP passes, the observed trend of the YS and UTS as well as FE is similar to that found at 373 K due to the softening factors already listed.

A collection of features observed on fracture surfaces of various tensile specimens is shown in Fig. 7. For the as extruded condition at room temperature, cleavage facets and steps as well as limited shallow dimples are the predominant features observed on the fracture surfaces. These features are substantially unaltered when considering all the ECAP-processed samples broken at room temperature. At the temperature of 373 K, the amount of observed dimples on the fracture surface of A samples increased consistently with the improved ductile behavior. As the number of ECAP passes increases, especially for 2P and 4P samples, the amount of plastic dimples observed on the fracture surface increased significantly and the observed dimples became deeper. Finally, at 423 K, even in the A samples, more dimples became evident. With increasing of number of ECAP passes, the fracture surfaces were almost completely covered by ductile dimples and some tearing edges emerged. These features are believed to be a clear indication for an enhancement of plasticity after ECAP at this temperature.

The compressive true stress vs true strain curves of various ECAP processed AZ80 alloy samples tested at different temperatures are shown in Fig. 8. Because of the initial fiber texture with the majority of the basal planes lying parallel to the compression axis and resulting in easy generation of {10-12} extension twins [31], sample A showed very low compressive yield strength. Nevertheless, with ECAP progress, YS progressively increases which is supposed to be mainly related to the grain boundary strengthening. At 373 K, apart from the sample subjected to 4 ECAP passes, the increasing trend of YS by ECAP advancement is confirmed. However, sample 4P exhibits slightly lower YS compared to 1P and 2P samples, while showing the highest elongation. Based on previous results collected on texture, it can be suggested that in 4P sample the particular basal plane orientation led to significant reduction of YS, implying that texture softening was the main deformation mechanism rather than grain refinement. This conclusion is in agreement with previous results showing that in Mg alloys, when the applied compressive load is parallel to basal planes, the deformation is dominated by {10-12} tensile twinning [32]. It should be also noted that grain size and texture have an important effect on the activation of tensile twinning [33]. In fine grain structure Mg alloys activation of extension twins is less favorable mainly due to the higher increasing rate of twinning stress than that of slip achieved with the decrease of

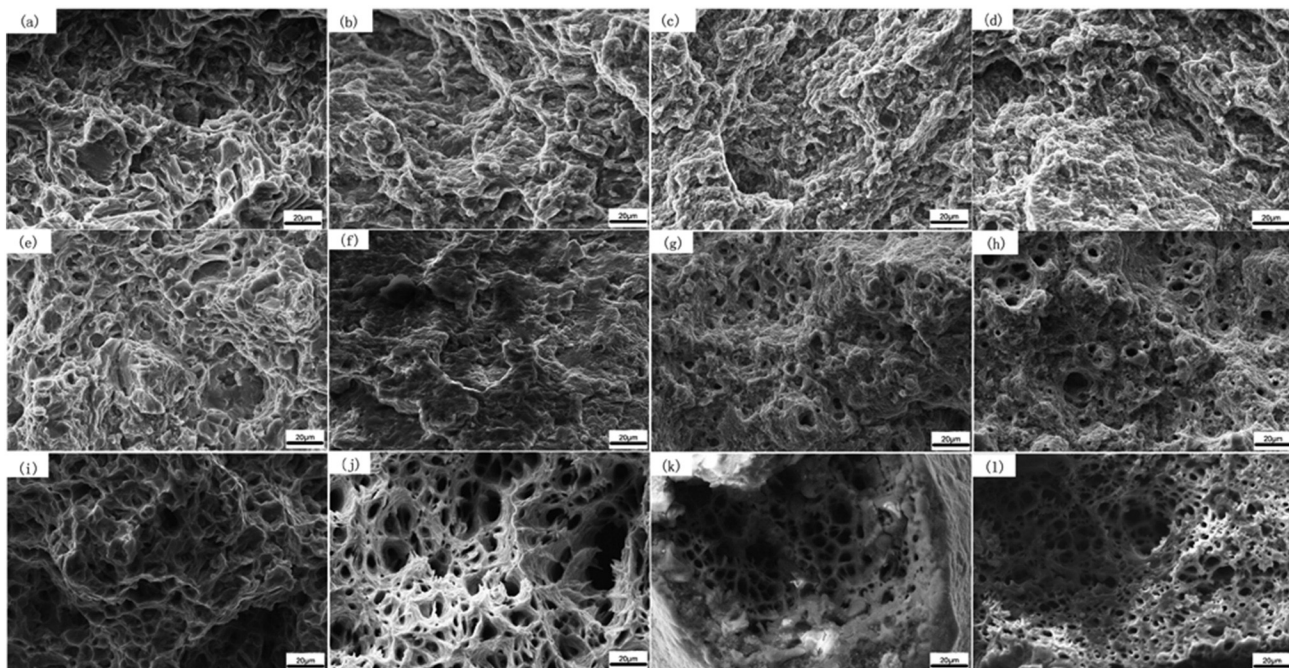


**Fig. 7.** Fracture surface appearance of various ECAP processed samples tensile tested under different temperatures. At RT: (a) A, (b) 1P, (c) 2P, (d) 4P; at 373 K: (e) A, (f) 1P, (g) 2P, (h) 4P; at 423 K: (i) A, (j) 1P, (k) 2P and (l) 4P;

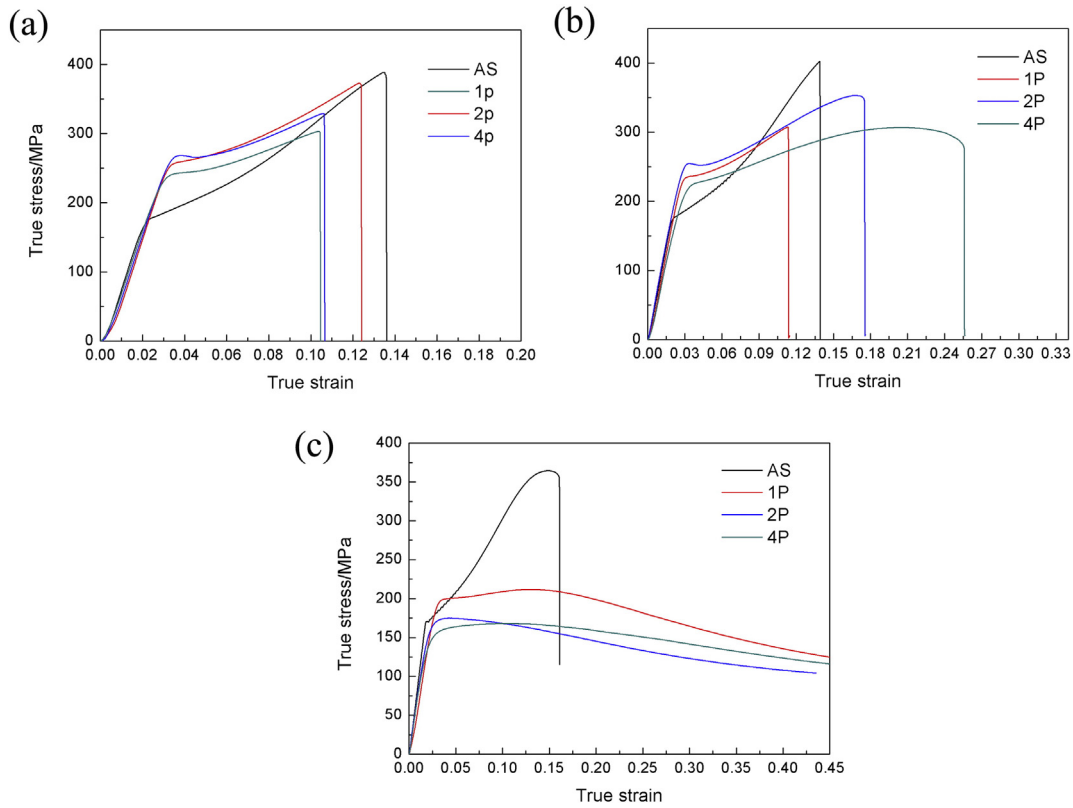


Fig. 8. Compressive true stress vs. true strain curves of AZ80 alloy processed by ECAP at different passes and tested at different temperatures: (a) RT, (b) 373 K, (c) 423 K.

grain size. Thus, the compressive strength improves after ECAP process due to the grain refinement. While due to the weakening of (0002) fiber texture, the Schmid factor of basal slips increases and the dislocation slips on basal planes would be much easier. Especially in 4P samples, the rotation of basal planes about  $45^\circ$  to ED makes basal slip more favorable. Besides, the CRSS of basal slips is smaller than {10-12} tensile twinning, resulting in a smaller compressive yield strength and higher ductility. At this condition, the softening effect induced by weakening texture plays a more important role than grain refinement. When the temperature increases to 423 K, the softening effect of orientation becomes more evident. The compressive strength decreases with increasing ECAP passes, while the fracture elongation concurrently increases.

### 3.3. Effects of ECAP process on tensile/compressive asymmetry of AZ80 Mg alloys at lower temperatures

Fig. 9 shows the compression-tension yield strength ratio (CYS/TYS) for all the samples investigated at different temperatures and ECAP passes. It can be seen that at RT this ratio continuously increases with ECAP progress, indicating that the tension-compression asymmetry is reduced by ECAP advancement. Moreover, at 373 K and 423 K CYS/TYS exceeds 1 for ECAP process samples implying that the compressive yield strength is larger than the tensile yield strength. The mentioned phenomenon was also observed in another research work. Yu et al. [34] employed ECAP process on AZ31 magnesium alloys. They measured a CYS value 36 MPa larger than the TYS in 4 pass samples, while the TYS was 50 MPa larger than CYS in as-received AZ31 magnesium alloy samples. This is mainly because the {10-12} tensile twinning dominates the deformation during compression and it becomes more difficult to be activated in fine grain structures [35]. On the other hand, due to refinement of grain size, non-basal slips and GBS might be active at 373 and 423 K during tension, resulting in decrease of tensile yield strength. In 4P samples, the (0002) basal planes are mostly oriented with an angle of  $45^\circ$  to the stress axis, thus making basal slips easier during compression. Furthermore, the CRSS of basal slip is smaller than {10-12} tensile twinning so that for 4P samples the CYS is lower than that found in 2P samples, leading to a lower tension-compression yield asymmetry.

Therefore, it can be stated that ECAP processing has an important role on the mechanical properties of AZ80 Mg alloys concerning tensile and compression mechanical behavior. At 423 K, grain refinement and texture softening induced by ECAP result in improved tensile ductility and compressive strength.

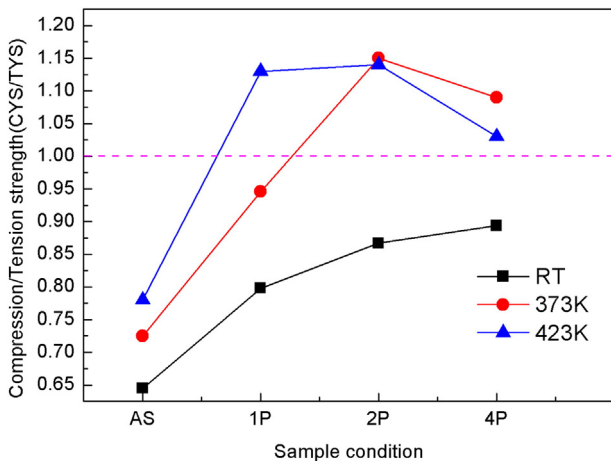


Fig. 9. Compression/tension yield strength ratio for the investigated samples as a function of temperature and ECAP passes.



## 4. Conclusions

In this paper, AZ80 Mg alloy was subjected to ECAP processing for 1, 2 and 4 passes at 523 K. Tensile and compressive tests were carried out at room temperature, 373 K and 423 K, to investigate mechanical properties of the material in the warm temperature range.

After ECAP passes, the grain size was significantly refined. The initial fiber texture gradually evolved into a new one featuring the preferential alignment of the basal planes along the ECAP shear planes.

The combined effects of texture and grain size as well as GBS played an important role on mechanical properties of AZ80 alloy. At room temperature, grain refinement induced by ECAP improved the measured strength. However, texture was found to be more important in the warm temperature range since at 373 K and 423 K GBS might be also activated and play an important role in the improvement of plasticity.

At elevated temperatures, due to the enhanced softening effect, the tensile strength decreased by ECAP progress. Nonetheless, the fracture elongation improved considerably and the tension-compression asymmetry notably reduced.

## Acknowledgments

This work is supported by the National Natural Science Foundation of China (51504162), National Natural Science Foundation of China (51375328), Shanxi Province Science Foundation for Youths (2015021073), Scientific and Technological Innovation Programs of Higher Education Institutions in Shanxi (2014118), and Fundamental Research Funds by Taiyuan University of Technology (tyut-rc201523a).

## References

- [1] M. Karami, R. Mahmudi, Hot shear deformation constitutive analysis and processing map of extruded Mg-12Li-1Zn bcc alloy, *Mater. Des.* 53 (2014) 534–539.
- [2] H. Zhang, G.S. Huang, J.F. Fan, H.J. Roven, B.S. Xu, H.B. Dong, Deep drawability and drawing behaviour of AZ31 alloy sheets with different initial texture, *J. Alloys Compd.* 615 (2014) 302–310.
- [3] J.A. Yasi, L.G. Hector, D.R. Trinkle, First-principles data for solid-solution strengthening of magnesium: from geometry and chemistry to properties, *Acta Mater.* 58 (2010) 5704–5713.
- [4] E. Mostaed, A. Fabrizi, D. Dellasega, F. Bonollo, M. Vedani, Microstructure, mechanical behavior and low temperature superplasticity of ECAP processed ZM21 Mg alloy, *J. Alloys Compd.* 638 (2015) 267–276.
- [5] Cao Z, Wang FH, Wan Q, Zhang ZY, Jin L, Dong J. Microstructure and mechanical properties of AZ80 magnesium alloy tube fabricated by hot flow forming, *Mater Des* 2015; 67: 64–71.
- [6] F. Li, X. Zeng, Q. Chen, G.J. Cao, Effect of local strains on the texture and mechanical properties of AZ31 magnesium alloy produced by continuous variable cross-section direct extrusion (CVCDE), *Mater. Des.* 85 (2015) 389–395.
- [7] K. Xia, J. Wang, X. Wu, G. Chen, M. Gurvan, Equal channel angular pressing of magnesium alloy AZ31, *Mater. Sci. Eng. A* 410 (2005) 324–327.
- [8] C.Y. Lin, H.J. Tsai, C.G. Chao, T.F. Liu, Effects of equal channel angular extrusion on the microstructure and high-temperature mechanical properties of ZA85 magnesium alloy, *J. Alloys Compd.* 530 (2012) 48–55.
- [9] W. Kim, S. Hong, Y. Kim, S. Min, H. Jeong, J. Lee, Texture development and its effect on mechanical properties of an AZ61 Mg alloy fabricated by equal channel angular pressing, *Acta Mater.* 51 (2003) 3293–3307.
- [10] G. Qiang, E. Mostaed, C. Zanella, Y. Zhentao, M. Vedani, Ultra-fine grained degradable magnesium for biomedical applications, *Rare Metal Mater. Eng.* 43 (2014) 2561–2566.
- [11] L. Lu, T. Liu, Y. Chen, L. Wang, Z. Wang, Double change channel angular pressing of magnesium alloys AZ31, *Mater. Des.* 35 (2012) 138–143.
- [12] K. Matsubara, Y. Miyahara, Z. Horita, T.G. Langdon, Achieving enhanced ductility in a dilute magnesium alloy through severe plastic deformation, *Metall. Mater. Trans. A* 35 (2004) 1735–1744.
- [13] S. Ion, F. Humphreys, S. White, Dynamic recrystallisation and the development of microstructure during the high temperature deformation of magnesium, *Acta Metall.* 30 (1982) 1909–1919.
- [14] S.R. Agnew, Ö. Duygulu, Plastic anisotropy and the role of non-basal slip in magnesium alloy AZ31B, *Int. J. Plast.* 21 (2005) 1161–1193.
- [15] J.A.D. Valle, O.A. Ruano, Influence of texture on dynamic recrystallization and deformation mechanisms in rolled or ECAPed AZ31 magnesium alloy, *Mater. Sci. Eng. A* 487 (2008) 473–480.
- [16] M. Ben-Haroush, G. Ben-Hamu, D. Eliezer, L. Wagner, The relation between micro-structure and corrosion behavior of AZ80 Mg alloy following different extrusion temperatures, *Corros. Sci.* 50 (2008) 1766–1778.
- [17] B. Mirzakhani, Y. Payandeh, Combination of severe plastic deformation and precipitation hardening processes affecting the mechanical properties in Al-Mg-Si alloy, *Mater. Des.* 68 (2015) 127–133.
- [18] Y. Tamura, Y. Kida, H. Tamehiro, N. Kono, H. Soda, A. McLean, The effect of manganese on the precipitation of Mg<sub>17</sub>Al<sub>12</sub> phase in magnesium alloy AZ 91, *J. Mater. Sci.* 43 (2008) 1249–1258.
- [19] X. Zhang, Y. Cheng, Tensile anisotropy of AZ91 magnesium alloy by equal channel angular processing, *J. Alloys Compd.* 622 (2015) 1105–1109.
- [20] J. He, T. Liu, S. Xu, Y. Zhang, The effects of compressive pre-deformation on yield asymmetry in hot-extruded Mg-3Al-1Zn alloy, *Mater. Sci. Eng. A* 579 (2013) 1–8.
- [21] H. Zhang, W. Jin, J. Fan, W. Cheng, H.J. Roven, B. Xu, H. Dong, Grain refining and improving mechanical properties of a warm rolled AZ31 alloy plate, *Mater. Lett.* 135 (2014) 31–34.
- [22] X.P. Luo, M.G. Zhang, Y.S. Chai, B. Li, J.Q. Zhou, Microstructure and mechanical properties of cast AZ81 magnesium alloy processed by equal channel angular pressing, *Mater. Sci. Technol.* 20 (2012) 72–76.
- [23] L. Balogh, R.B. Figueiredo, T. Ungár, T.G. Langdon, The contributions of grain size, dislocation density and twinning to the strength of a magnesium alloy processed by ECAP, *Mater. Sci. Eng. A* 528 (2010) 533–538.
- [24] R. Gehrmann, Frommert, M.M. Gottstein G. Texture effects on plastic deformation of magnesium, *Mater. Sci. Eng. A* 395 (2005) 338–349.
- [25] N. Li, G. Huang, X. Zhong, Q. Liu, Deformation mechanisms and dynamic recrystallization of AZ31 Mg alloy with different initial textures during hot tension, *Mater. Des.* 50 (2013) 382–391.
- [26] B. Song, G. Huang, H. Li, L. Zhang, G. Huang, F. Pan, Texture evolution and mechanical properties of AZ31B magnesium alloy sheets processed by repeated unidirectional bending, *J. Alloys Compd.* 489 (2010) 475–481.
- [27] J. Wang, D.X. Zhang, Y. Li, Z.Y. Xiao, J.P. Fouse, X.Y. Yang, Effect of initial orientation on the microstructure and mechanical properties of textured AZ31 Mg alloy during torsion and annealing, *Mater. Des.* 86 (2015) 526–535.
- [28] J. Ma, X. Yang, Q. Huo, H. Sun, J. Qin, J. Wang, Mechanical properties and grain growth kinetics in magnesium alloy after accumulative compression bonding, *Mater. Des.* 47 (2013) 505–509.
- [29] Koike J, Kobayashi T, Mukai T, Watanabe H, Suzuki M, Maruyama K, Higashi K. The activity of non-basal slip systems and dynamic recovery at room temperature in fine-grained AZ31B magnesium alloys. *Acta Mater* 2003; 51:2055–2065.
- [30] S. Yi, S. Zaefferer, H.G. Brokmeier, Mechanical behaviour and microstructural evolution of magnesium alloy AZ31 in tension at different temperatures, *Mater. Sci. Eng. A* 424 (2006) 275–281.
- [31] H. Zhang, Y. Liu, J. Fan, H.J. Roven, W. Cheng, B. Xu, H. Dong, Microstructure evolution and mechanical properties of twinned AZ31 alloy plates at lower elevated temperature, *J. Alloys Compd.* 615 (2014) 687–692.
- [32] L. Wang, G. Huang, Q. Quan, P. Bassani, V.M. Mostaed, F. Pan, The effect of twinning and detwinning on the mechanical property of AZ31 extruded magnesium alloy during strain-path changes, *Mater. Des.* 63 (2014) 177–184.
- [33] H. Fan, S. Aubry, A. Arsenlis, J.A. El-Awady, Orientation influence on grain size effects in ultrafine-grained magnesium, *Scr. Mater.* 97 (2015) 25–28.
- [34] X. Yu, Y. Li, Q.M. Wei, Y.Z. Guo, T. Suo, F. Zhao, Microstructure and mechanical behavior of ECAP processed AZ31B over a wide range of loading rates under compression and tension, *Mech. Mater.* 86 (2015) 55–70.
- [35] R. Sánchez-Martín, M. Pérez-Prado, J. Segurado, J. Molina-Aldareguia, Effect of indentation size on the nucleation and propagation of tensile twinning in pure magnesium, *Acta Mater.* 93 (2015) 114–128.